Title
Negative viscosity from negative compressibility and axial flow shear stiffness in a straight magnetic field

Journal
Physics of Plasmas, 24(3)

ISSN
1070-664X

Authors
Li, JC
Diamond, PH

Publication Date
2017-03-01

DOI
10.1063/1.4978956

Negative viscosity from negative compressibility and axial flow shear stiffness in a straight magnetic field

J. C. Li and P. H. Diamond

Citation: Physics of Plasmas **24**, 032117 (2017); doi: 10.1063/1.4978956
View online: http://dx.doi.org/10.1063/1.4978956
View Table of Contents: http://aip.scitation.org/toc/php/24/3
Published by the American Institute of Physics

Negative viscosity from negative compressibility and axial flow shear stiffness in a straight magnetic field

J. C. Li and P. H. Diamond
CMTFO and CASS, University of California, San Diego, California 92093, USA

(Received 24 December 2016; accepted 8 March 2017; published online 23 March 2017)

Negative compressibility ion temperature gradient (ITG) turbulence in a linear plasma device controlled shear de-correlation experiment can induce a negative viscosity increment. However, even with this negative increment, we show that the total axial viscosity remains positive definite, i.e., no intrinsic axial flow can be generated by pure ITG turbulence in a straight magnetic field. This differs from the case of electron drift wave turbulence, where the total viscosity can turn negative, at least transiently. When the flow gradient is steepened by any drive mechanism, so that the parallel shear flow instability (PSFI) exceeds the ITG drive, the flow profile saturates at a level close to the value above which PSFI becomes dominant. This saturated flow gradient exceeds the PSFI linear threshold, and grows with ∇T_{i0} as $|\nabla V_\parallel|/|k_\parallel c_s| \sim |\nabla T_{i0}|^{2/3}/(k_\parallel T_{i0})^{2/3}$. This scaling trend characterizes the effective stiffness of the parallel flow gradient. *Published by AIP Publishing.* [http://dx.doi.org/10.1063/1.4978956]

I. INTRODUCTION

Strong toroidal rotation and weak magnetic shear are desirable for enhanced confinement in tokamaks. External drives for rotation, e.g., neutral beams, will be insufficient to assure MHD stability[1] in future fusion devices, such as ITER. Thus, intrinsic rotation is of interest. Weak or reversed magnetic shear has long been known to enhance microstability and confinement. Studies on enhanced reversed shear,[2] negative central shear,[3] weakly negative shear,[4] etc., reveal this trend. For example, de-stiffened states, with enhanced confinement, were observed in the weak shear regime in JET.[5] Therefore, intrinsic rotation at weak magnetic shear is of particular interest. Intrinsic rotation can be generated by background turbulence. Thus, in tokamaks, intrinsic rotation usually tracks the driving gradient of turbulence.[6] This also poses the question of how the flow gradient (∇V_ϕ) interacts with, and scales with, the driving gradient of turbulence (i.e., edge ion temperature gradient (ITG) in the case of Ref. 6).

The controlled shear de-correlation experiment (CSDX) is a cylindrical linear device with uniform axial magnetic fields and turbulence driven intrinsic parallel flows. It offers a well-diagnosed venue for the study of intrinsic flows in the shear-free regime.[7] Since most mechanisms for intrinsic parallel flow generation rely on magnetic shear,[8] a new dynamical symmetry breaking mechanism was proposed to account for axial flow generation in CSDX. This mechanism does not require a specific magnetic field configuration, so it can work in regimes with and without shear. Symmetry breaking is usually required to set a preferred direction for the flow, i.e., a finite $\langle k_\parallel \rangle$. The residual stress is determined by the correlator $\langle k_\theta k_\parallel \rangle \equiv \sum_k k_\theta k_\parallel |\phi_k|^2$. Hence, asymmetry-specifically, handedness-in the turbulent spectrum ($|\phi_k|^2$) is required to obtain a nonzero residual stress. In CSDX, where the turbulence is usually a population of electron drift waves (EDWs), the growth/drive rate is determined by the drift mode frequency shift relative to the electron drift frequency, i.e., $\gamma_k \sim \omega_{*e} - \omega_k$.[9] A test flow shear ($\delta V_\parallel'$) changes the frequency shift, setting modes with $k_\parallel k_\theta \delta V_\parallel' > 0$ to grow faster than those with $k_\parallel k_\theta \delta V_\parallel' < 0$. Therefore, a spectral imbalance in $k_\parallel k_\theta$ space develops, which sets a finite residual stress $\delta \Pi_{r\parallel}^{Res}$. The resulting residual stress drives an intrinsic flow, and so reinforces the test flow shear. This self-amplification of $\delta V_\parallel'$ is a negative viscosity phenomenon. The residual stress induces a negative viscosity increment, i.e., $\delta \Pi_{r\parallel}^{Res} \sim |\chi_\phi^{Res}| \delta V_\parallel'$. The basic scenario resembles that familiar from the theory of zonal flow generation.[10] The flow shear modulation ($\delta V_\parallel'$) becomes unstable when the total viscosity $\chi_\phi^{Tot} = \chi_\phi - |\chi_\phi^{Res}|$ turns negative. Therefore, $\delta V_\parallel'$ can be self-reinforced via modulational instability. When the flow profile gradient steepens enough, so that the parallel shear flow instability (PSFI) is turned on, the mean flow gradient ($\nabla V_\parallel$) saturates at the PSFI linear threshold and the total viscosity stays positive, due to the contribution induced by PSFI, i.e., $\chi_\phi^{Tot} = \chi_\phi^{DW} + \chi_\phi^{PSFI} - |\chi_\phi^{Res}|$. In CSDX, the PSFI linear threshold grows as $|V_\parallel'|_{\rm crit}/|k_\parallel c_s| \sim (k_\parallel L_n)^{-2}$,[9,11] where $L_n \equiv -(\partial_r \ln n_0)^{-1}$. Therefore, the flow gradient tracks the turbulence driving gradient (i.e., ∇n_0) as $\nabla V_\parallel/|k_\parallel c_s| \sim |V_\parallel'|_{\rm crit}/|k_\parallel c_s| \sim (k_\parallel L_n)^{-2}$. This scaling motivates us to wonder if there is a generalized form of the Rice-type scaling.[6,12]

CSDX has straight magnetic fields, and thus is an important limiting case for understanding flow generation at zero shear. While existing models of axial flow generation in CSDX are based on EDW turbulence, fluctuations propagating in the ion drift direction are observed.[13] Such ion features appear in the central region of the cylindrical plasma in CSDX, where the density profile is flat. In addition, turbulence driven by the ion temperature gradient (ITG) controls momentum transport in tokamaks operated in enhanced

confinement states, e.g., states with an internal transport barrier (ITB). Also, intrinsic rotation tracks the edge temperature gradient.[6] These trends beg the questions:

- How does negative compressibility turbulence, e.g., ITG turbulence, affect momentum transport at zero magnetic shear? Particularly, what happens in flat density limit?
- How does $\nabla V_\parallel$ saturate in ITG turbulence?
- With tokamaks in mind, how does this new mechanism interact with conventional mechanisms which exploit magnetic shear? What is the interplay of $\nabla V_\parallel$ and ∇T_{i0}?

It has long been known that a finite parallel shear flow (PSF) $\nabla V_\parallel$ can enhance ITG turbulence in sheared magnetic fields.[14] However, the detailed question of how the mean flow gradient, $\nabla V_\parallel$, and its perturbation, $\delta V_\parallel'$, affect flow generation and saturation in ITG turbulence in a straight field remains unanswered.

In this paper, we study the effects of ITG turbulence on momentum transport in a straight magnetic field. In the regime well above the ITG stability boundary, a perturbation to the flow profile, $\delta V_\parallel'$, can reduce the turbulent viscosity. $\delta V_\parallel'$ breaks the symmetry by allowing modes with $k_\theta k_\parallel \delta V_\parallel' > 0$ to grow faster than modes with $k_\theta k_\parallel \delta V_\parallel' < 0$. This results in a spectral imbalance in $k_\theta k_\parallel$ space. The residual stress set by this spectral imbalance drives an up-gradient momentum flux which induces a negative viscosity increment, i.e., $\delta\Pi_{r\parallel}^{Res} \sim |\chi_\phi^{Res}|\delta V_\parallel'$ with $\chi_\phi^{Res} < 0$. Thus, the *total* viscosity is reduced, since $\chi_\phi^{Tot} = \chi_\phi - |\chi_\phi^{Res}|$. The mean flow gradient driven by ITG turbulence is consequently steepened, since $\nabla V_\parallel \sim \Pi_{r\parallel}^{Res}/\chi_\phi^{Tot}$.

However, unlike the case of dynamical symmetry breaking in EDW turbulence, we show that symmetry breaking induced by $\delta V_\parallel'$ in ITG turbulence alone *cannot* amplify the seed flow shear ($\delta V_\parallel'$). Therefore, ITG turbulence *cannot* drive intrinsic flows in straight magnetic fields. In ITG turbulence, the total momentum diffusivity χ_ϕ^{Tot} remains positive, because $|\chi_\phi^{Res}| = \frac{1}{3}\chi_\phi$. The growth rate of a flow shear modulation is $\gamma_q = -\chi_\phi^{Tot} q_r^2$, where q_r is the radial mode number of the modulation. A positive definite χ_ϕ^{Tot} does not induce modulational instability. This differs from the case of EDW turbulence. Table I shows the comparison between symmetry breaking in ITG and EDW turbulence.

The axial flow in CSDX can be driven by various external sources. The axial ion pressure drop, induced by the location of the heating source on one end of the cylindrical plasma, can drive an axial flow. Biasing the end plate can also accelerate axial ion flows by axial electric fields.

TABLE I. Comparison of $\delta V_\parallel'$ induced symmetry breaking in ITG turbulence and electron drift wave turbulence. The total viscosity, $\chi_\phi^{Tot} = \chi_\phi + \chi_\phi^{Res}$, determines the modulational growth rate of $\delta V_\parallel'$ which is $\gamma_q = -\chi_\phi^{Tot} q_r^2$ with q_r being the radial mode number of the shear modulation $\delta V_\parallel'$.

	ITG turbulence	Electron drift wave
Direction of correlator	$\langle k_\theta k_\parallel\rangle \delta V_\parallel' > 0$	$\langle k_\theta k_\parallel\rangle \delta V_\parallel' > 0$
Viscosity increment by $\delta\Pi_{r\parallel}^{Res}$	$\chi_\phi^{Res} < 0$	$\chi_\phi^{Res} < 0$
Total viscosity χ_ϕ^{Tot}	Positive	Can be negative
Modulations	Stable	Can be unstable

The flow gradient produced by external or intrinsic drive ultimately must saturate due to PSFI-induced relaxation. $\nabla V_\parallel$ can be enhanced by external drives, e.g., the axial ion pressure drop and end plate biasing. When $\nabla V_\parallel$ is stronger than the ion temperature profile gradient (∇T_{i0}), PSFI drive controls the turbulence. Here, the relative strength between ∇T_{i0} and $\nabla V_\parallel$ is measured by the relative length scale $L_T/L_V \equiv \partial_r \ln V_\parallel/\partial_r \ln T_{i0}$. In turbulence controlled by PSFI, both the residual stress and turbulent viscosity depend nonlinearly on $\nabla V_\parallel$. As a result, the flow gradient saturates *above* the linear threshold of PSFI and the saturated $\nabla V_\parallel$ grows with ∇T_{i0}. This implies a "stiff" $\nabla V_\parallel$ profile. An aim of this paper is to calculate the scaling $\nabla V_\parallel/k_\parallel c_s \sim (k_\parallel L_T)^{-\alpha}$ of this stiffness.

The scaling of the $\nabla V_\parallel$ profile stiffness reveals the final state of the nonlinear interaction between $\nabla V_\parallel$ and ∇T_{i0}. It should be noted that PSFI co-exists with ITG turbulence. Their relative strength depends on L_T/L_V. Because $\nabla V_\parallel$ and ∇T_{i0} are coupled nonlinearly, they do not simply add up. However, PSFI can be distinguished from ITG instability (at least in simulation) by comparing their mode phases. The mode phase is defined as

$$\theta_k \equiv \begin{cases} \tan^{-1}(\gamma_k/\omega_k), & \omega_k > 0; \\ \pi + \tan^{-1}(\gamma_k/\omega_k), & \omega_k < 0. \end{cases}$$

Here, γ_k and ω_k are the growth rate and real frequency of the mode. PSFI has zero frequency, which means $\theta_k^{PSFI} = \pi/2$, while the ITG mode phase is usually $\theta_k^{ITG} = 2\pi/3$. The theoretical concept of mode phase is related to the cross phase between flow fluctuations, $\tilde{v}_\parallel$ and $\tilde{v}_r$, and thus can be measured in experiments, at least in principle. Also, since mode phase affects Reynolds stress $\langle \tilde{v}_\parallel \tilde{v}_r\rangle$, intrinsic flow profiles are sensitive to the mode phase.

Comparison between symmetry breaking in EDW and ITG turbulence drives us to wonder if flow reversal is possible in CSDX by a change in turbulence population from EDW to ITG? More generally, can the idea that mode change leads to flow reversals[15] be tested by basic experiments? The flow profile in CSDX is determined by the ratio between the axial ion pressure drop ΔP_i and the total turbulent viscosity,[9] i.e., $V_\parallel \sim \int_r^a dr \Delta P_i/\chi_\phi^{Tot}$, where a is the plasma radius in CSDX. In EDW, although χ_ϕ^{Tot} can turn negative at least transiently, it is finally forced positive by PSFI saturation. In ITG turbulence, χ_ϕ^{Tot} is positive definite, since $|\chi_\phi^{Res}| = \frac{1}{3}\chi_\phi$. Therefore, there would be no argument for flow reversal in the final state, even though fluctuation or reversal may occur as a transient. Also, one can argue that flow reversal, even if it exists in CSDX, does not track the change in turbulence from EDW to ITG.

We neglect the momentum pinch effect in this work. In addition to the diffusive and residual components, the parallel Reynolds stress can have a momentum pinch term that is proportional to the flow magnitude. Since the momentum pinch is usually due to the toroidal effect in tokamaks,[16–18] it is neglected in this work, where we study linear devices that

have straight and uniform magnetic fields. In general, the momentum pinch is of the turbulent equipartition variety, and so $|V_{pinch}|/|\chi_\phi| \sim 1/R_0$, where R_0 is the major radius of the tokamak. This is explained as a toroidal effect. It is possible to also have L_n scalings, i.e., $|V_{pinch}|/|\chi_\phi| \sim 1/L_n$, in certain parameter regimes. However, since this analysis does not treat self-consistent evolution of density profiles, we decided to omit a discussion of this rather sensitive, detailed effect.

The rest of this paper is organized as follows: Sec. II introduces the fluid model of the PSF-ITG system into a straight magnetic field. Sec. III discusses the three regimes that we consider in this work. Sec. IV summarizes the structure of results. Sec. V presents results on mode phase, symmetry breaking, and flow profile in each regime. Finally, Sec. VI summarizes and discusses the results.

II. FLUID MODEL FOR THE PSF-ITG SYSTEM

We consider a system where the ion temperature gradient (∇T_{i0}) is coupled to the flow gradient ($\nabla V_\parallel$), i.e., a coupled PSF-ITG system of potential vorticity, $\tilde{q} = (1-\nabla_\perp^2)\phi$, parallel flow, $v_\parallel = \tilde{v}_\parallel + V_\parallel$, and ion pressure, $p_i = \tilde{p}_i + P_0$, with zero magnetic shear in cylindrical geometry

$$\frac{d}{dt}\left(1-\nabla_\perp^2\right)\phi + \mathbf{v}_E\cdot\frac{\nabla n_0}{n_0} + \nabla_\parallel \tilde{v}_\parallel = 0, \tag{1}$$

$$\frac{d\tilde{v}_\parallel}{dt} + \mathbf{v}_E\cdot\nabla V_\parallel = -\nabla_\parallel\phi - \nabla_\parallel\tilde{p}_i, \tag{2}$$

$$\frac{d\tilde{p}_i}{dt} + \frac{1}{\tau}\mathbf{v}_E\cdot\frac{\nabla P_0}{P_0} + \frac{\Gamma}{\tau}\nabla_\parallel\tilde{v}_\parallel + \nabla_\parallel Q_\parallel = 0. \tag{3}$$

Here, lengths are normalized by $\rho_s \equiv \sqrt{m_i T_{e0}}/(eB_0)$, time is normalized by the ion cyclotron frequency ω_{ci}^{-1}, velocities are normalized by the ion sound speed $c_s \equiv \sqrt{T_{e0}/m_i}$, and the electrostatic potential is normalized as $\phi \equiv e\tilde{\varphi}/T_{e0}$. The convective derivative is defined as $d/dt \equiv \partial/\partial t + \mathbf{v}_E\cdot\nabla$, where $\mathbf{v}_E = \mathbf{B}_0\times\nabla\phi/B_0$ is the $E\times B$ velocity. The kinetic effect of Landau damping is retained by including the parallel heat flux, with Hammett-Perkins closure $Q_{\parallel,k} = -\chi_\parallel n_0 i k_\parallel \tilde{T}_{i,k}$. Here, the (collisionless) parallel heat conductivity is $\chi_\parallel = 2\sqrt{2}v_{Thi}/(\sqrt{\pi}|k_\parallel|)$, and v_{Thi} is the ion thermal speed. The ratio of specific heats is $\Gamma = 3$ in this model. The electron response is adiabatic, corresponding to Boltzmann electrons, i.e., $\tilde{n} = \phi$. Hence, $\tilde{p}_i = \tilde{T}_i + \phi/\tau$, with the temperature ratio defined as $\tau \equiv T_{e0}/T_{i0}$. Since the ion features exist in the center of CSDX where the density profile is flat, we take $\nabla n_0 = 0$ throughout. Thus, the mean pressure gradient consists of only a temperature gradient, i.e., $\nabla P_0 = \nabla T_{i0}$. The linear dispersion relation for the PSF-ITG system is

$$A\Omega^3 - (C_0 - V')\Omega - D + \frac{i|k_\parallel|\chi_\parallel}{c_s}\left(A\Omega^2 + V' - \frac{1+\tau}{\tau}\right) = 0, \tag{4}$$

with $\Omega \equiv \omega/|k_\parallel c_s|$, $V' \equiv k_\theta k_\parallel \rho_s c_s V_\parallel'/k_\parallel^2 c_s^2$, $A \equiv 1 + k_\perp^2\rho_s^2$, $C_0 \equiv 1 + (1+k_\perp^2\rho_s^2)\Gamma/\tau$, $D \equiv \omega_T/\tau|k_\parallel c_s|$. ω_T is defined as $\omega_T \equiv -k_\theta\rho_s c_s \partial_r \ln T_{i0}$. In a linear device, such as CSDX, $\tau > 1$, so $|k_\parallel|\chi_\parallel/c_s \sim 1/\sqrt{\tau} < 1$. Thus, terms involving $i|k_\parallel|\chi_\parallel/c_s$ will be neglected.

∇T_{i0} and $\nabla V_\parallel$ are coupled nonlinearly, because either ∇T_{i0} or $\nabla V_\parallel$ can drive instability, by forcing

$$\Delta \equiv \left(\frac{D}{2A}\right)^2 - \left(\frac{C_0 - V'}{3A}\right)^3 > 0. \tag{5}$$

The growing mode has growth rate and frequency

$$\gamma_k = \frac{\sqrt{3}}{2}|k_\parallel c_s|\left(\sqrt[3]{\frac{D}{2A}+\sqrt{\Delta}} - \sqrt[3]{\frac{D}{2A}-\sqrt{\Delta}}\right), \tag{6}$$

$$\omega_k = -\frac{1}{2}|k_\parallel c_s|\left(\sqrt[3]{\frac{D}{2A}+\sqrt{\Delta}} + \sqrt[3]{\frac{D}{2A}-\sqrt{\Delta}}\right). \tag{7}$$

In Sec. V, we will see that in the presence of a shear flow $V_\parallel'$, modes with $k_\theta k_\parallel V_\parallel' > 0$ grow faster than others. Therefore, we take $V' \equiv k_\theta k_\parallel V_\parallel'/k_\parallel^2 c_s^2 > 0$.

The underlying instability drive is negative compressibility. Both ITG instability and PSFI are negative compressibility phenomena. Negative compressibility means that an increase in density (compression in volume) leads to a decrease in pressure. For the system studied here, the relation between the pressure perturbation and density perturbation is

$$\tilde{p}_i \sim \left(\frac{\Gamma}{\tau}\frac{k_\parallel^2 c_s^2}{\omega_k^2} - \frac{\Gamma}{\tau}\frac{k_\theta k_\parallel \rho_s c_s V_\parallel'}{\omega_k^2} - \frac{\omega_T}{\tau|\omega_k|}\right)\tilde{n}.$$

Here, we have used the adiabatic electron response $\tilde{n} \sim \phi_k$. The compressibility becomes negative when either of ITG instability or PSFI is above the threshold. Note that ∇T_{i0} and $\nabla V_\parallel$ can act in synergy to turn the compressibility negative, driving the system unstable.

Although coupled nonlinearly, PSFI and ITG instability can be distinguished by different mode phases. PSFI is a purely growing mode, so $\theta_k = \pi/2$. This is because (for $\nabla T_{i0} \to 0$), the dispersion relation becomes

$$A\Omega^2 - (C_0 - V') = 0, \tag{8}$$

which gives a purely growing branch when $V' > V'_{\rm crit} \equiv C_0$, with growth rate $\gamma_k = |k_\parallel c_s|\sqrt{(V'-C_0)/A}$. In contrast, ITG instability has a negative real frequency whose magnitude is comparable to the growth rate. If ∇T_{i0} (the term D) dominates the dispersion relation Eq. (4), then the resulting ITG mode has complex frequency $\omega \sim \exp(i2\pi/3)[|\omega_T|k_\parallel^2 c_s^2/(\tau A)]^{1/3}$, with mode phase $\theta_k \cong 2\pi/3$.

III. INSTABILITY REGIMES

The nonlinear coupling between $\nabla V_\parallel$ and ∇T_{i0} significantly increases the level of complexity of calculating the residual stress and the flow profile. Therefore, we classify the PSF-ITG system into three regimes (Fig. 1), determined by length scales $L_V^{-1} \equiv -\partial_r \ln V_\parallel$ and $L_T^{-1} \equiv -\partial_r \ln T_{i0}$

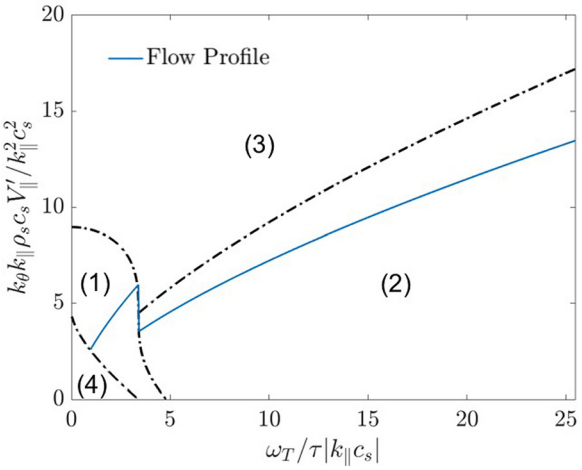

FIG. 1. Regime defined by instability types and flow profile driven by the PSF-ITG turbulence. The regimes are (1) marginal regime; (2) ITG regime; (3) PSFI regime; and (4) stable regime. Parameters used for this plot are $k_\theta \rho_s = 0.4$ and the ratio of specific heats $\Gamma = 3$.

(1) The marginal regime is defined by $\Delta \gtrsim 0$, where PSFI and ITG instability co-exist, and both of them are weakly unstable. Thus, $\nabla V_\parallel$ and ∇T_{i0} are nonlinearly coupled in this regime.
(2) The ITG regime is where the system is well above the marginal state and ∇T_{i0} contributes more than $\nabla V_\parallel$ to the magnitude of Δ, i.e., $(D/2A)^2 > (V'/3A)^3$ which leads to

$$\frac{L_T^{2/3}}{|k_\parallel|^{1/3} L_V} < \frac{c_s}{V_\parallel} \frac{3}{2^{2/3}} \frac{A^{1/3}}{(k_\theta \rho_s)^{1/3} \tau^{2/3}}. \tag{9}$$

We show in Sec. V that, in this regime, although a test flow shear $\delta V'_\parallel$ induces a negative viscosity contribution, the *total viscosity* is *positive definite*. Consequently, there is no intrinsic flow driven by ITG turbulence in a straight field. This is quite different from the case of EDW turbulence.
(3) The PSFI regime is also well above the marginal state, but where $\nabla V_\parallel$ contributes more than ∇T_{i0} to instability drive, i.e.,

$$\frac{L_T^{2/3}}{|k_\parallel|^{1/3} L_V} > \frac{c_s}{V_\parallel} \frac{3}{2^{2/3}} \frac{A^{1/3}}{(k_\theta \rho_s)^{1/3} \tau^{2/3}}. \tag{10}$$

This gives the regime boundary above which PSFI controls the turbulence

$$|V'_\parallel|_{\text{reg}} = \frac{3}{2^{2/3}} A^{1/3} \left(\frac{|\omega_T|}{\tau |k_\parallel c_s|} \right)^{2/3} \frac{|k_\parallel| c_s}{k_\theta \rho_s}. \tag{11}$$

External flow drives can enhance the flow profile gradient. Hence, $\nabla V_\parallel$ can exceed the PSFI regime boundary ($|V'_\parallel|_{\text{reg}}$). PSFI is nonlinear in $\nabla V_\parallel$. Consequently, the turbulent viscosity is nonlinear in $\nabla V_\parallel$, and so $\nabla V_\parallel$ saturates at $|V'_\parallel|_{\text{reg}}$ which is *above the linear threshold of PSFI*. Thus, there is a clear distinction between the threshold $\nabla V_\parallel$ profile and the saturated-or "stiff"-$\nabla V_\parallel$ profile.

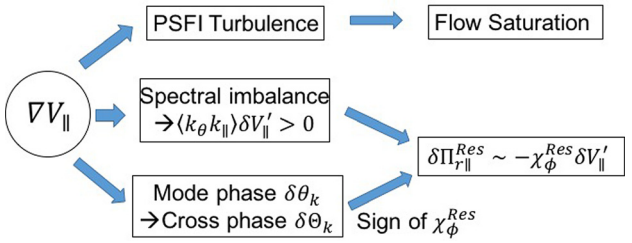

FIG. 2. Diagram of the three roles played by $\nabla V_\parallel$ in the PSF-ITG system.

IV. STRUCTURE OF RESULTS

In this section, we summarize the key aspects of results (Fig. 2). We consider (a) symmetry breaking by $\delta V'_\parallel$, (b) mode phase, and c) flow profile in each of the three regimes. A test flow shear $\delta V'_\parallel$ can break the symmetry and induce a incremental viscosity via the residual stress, i.e., $\delta \Pi_{r\parallel}^{Res} = -\chi_\phi^{Res} \delta V'_\parallel$. The sign of χ_ϕ^{Res} is determined by the mode phase. Thus, χ_ϕ^{Res} has different signs in PSFI and ITG turbulence. Finally, we need to calculate the flow profile, in order to explore possibilities about flow saturation in the context of negative compressibility turbulence, i.e., ITG and PSFI turbulence. In the rest of the section, we discuss these three aspects in detail.

A. Symmetry breaking by $\delta V'_\parallel$

A perturbation to the flow profile, $\delta V'_\parallel$, breaks the $k_\parallel \rightarrow -k_\parallel$ symmetry. $\langle k_\theta k_\parallel \rangle$ is linked to $\delta V'_\parallel$ via the acoustic coupling, $\nabla_\parallel \tilde{v}_\parallel$. In Sec. V, we will show that modes with $k_\theta k_\parallel \delta V'_\parallel > 0$ grow faster than those without. This sets a spectral imbalance in $k_\theta k_\parallel$ space. Further, the finite residual stress set by this imbalance is found to be a Fickian momentum flux, i.e., $\delta \Pi_{r\parallel}^{Res} \sim -\chi_\phi^{Res} \nabla V_\parallel$. The viscosity increment induced by residual stress then adds to the total viscosity, so that $\chi_\phi^{Tot} = \chi_\phi + \chi_\phi^{Res}$. Table II compares symmetry breaking in the three regimes.

TABLE II. Characteristics of the three PSF-ITG instability regimes. Mode phase is defined as the phase of complex mode frequency, i.e., $\omega \equiv \omega_k + i\gamma_k \equiv |\omega| e^{i\theta_k}$. $\delta\theta_k$ is the phase of perturbed complex frequency, $\delta\omega$, due to $\delta V'_\parallel$. χ_ϕ^{Res} is the incremental viscosity induced by $\delta V'_\parallel$. Since PSFI is driven by $\nabla V_\parallel$ nonlinearly, the $\delta V'_\parallel$ effect is nonlinear, so we do not consider its linear effects, i.e., $\delta\theta_k$ and χ_ϕ^{Res}.

	Marginal regime	ITG regime	PSFI regime
Primary turbulence drive	∇T_{i0} and $\nabla V_\parallel$	∇T_{i0}	$\nabla V_\parallel$
$\delta V'_\parallel$ induced spectral imbalance	$\langle k_\theta k_\parallel \rangle \delta V'_\parallel > 0$	$\langle k_\theta k_\parallel \rangle \delta V'_\parallel > 0$	$\langle k_\theta k_\parallel \rangle \delta V'_\parallel > 0$
Mode phase θ_k	$\lesssim \pi$	$2\pi/3$	$\gtrsim \pi/2$
Perturbed mode phase $\delta\theta_k$	$\pi/2$	$\pi/3$	NA
Sign of χ_ϕ^{Res}	$\chi_\phi^{Res} > 0$	$\chi_\phi^{Res} < 0$	NA

B. Mode phase

The sign of residual stress is determined by mode phase. Here, mode phase (θ_k) is defined as the phase of the complex mode frequency, i.e., $\omega = \omega_k + i\gamma_k \equiv e^{i\theta_k}\sqrt{\omega_k^2+\gamma_k^2}$. Linearizing the response of $\tilde{v}_{\parallel,k}$, we can obtain the quasilinear Reynolds stress[19,20]

$$\langle \tilde{v}_\parallel | \tilde{v}_r \rangle = -\chi_\phi V_\parallel' + \Pi_{r\parallel}^{Res}, \tag{12}$$

with the turbulent viscosity

$$\chi_\phi \approx \Re \sum_k \frac{i}{\omega} k_\theta^2 \rho_s^2 |\phi_k|^2, \tag{13}$$

and residual stress

$$\Pi_{r\parallel}^{Res} \approx \Re \sum_k \frac{i}{\omega^2}\frac{\omega_T}{\tau} k_\theta k_\parallel \rho_s c_s |\phi_k|^2, \tag{14}$$

where $\omega_T \equiv -k_\theta \rho_s c_s \partial_r T_{i0}/T_{i0}$. Here, $\omega \equiv \omega_k + i\gamma_k = |\omega| e^{i\theta_k}$ is the complex mode frequency with mode number k, and so $i/\omega \sim e^{i(\pi/2-\theta_k)}$ and $i/\omega^2 \sim e^{i(\pi/2-2\theta_k)}$. Therefore, the *sign* of the residual stress is determined by θ_k, as $\Pi_{r\parallel}^{Res} \sim \langle k_\theta k_\parallel \rangle \Re(i/\omega^2) \sim \langle k_\theta k_\parallel \rangle \cos(\pi/2 - 2\theta_k)$.

Mode phase also determines the sign of χ_ϕ^{Res}, i.e., the viscosity contribution induced by residual stress. In the presence of a test flow shear, $\delta V_\parallel'$, the residual stress induces a momentum flux, $\delta\Pi_{r,\parallel}^{Res} = -\chi_\phi^{Res}\delta V_\parallel'$. The sign of χ_ϕ^{Res} is determined by both the mode phase and its change due to $\delta V_\parallel'$. The residual stress' response to the test flow shear is

$$\delta\Pi_{r,\parallel}^{Res} \sim -2\sum_k \cos\left(\frac{\pi}{2} + \delta\theta_k - 3\theta_k\right)\frac{|\delta\omega|}{|\omega|^3}\frac{\omega_T}{\tau} k_\theta k_\parallel |\phi_k|^2, \tag{15}$$

where $\delta\theta_k$ is the phase of perturbed complex frequency due to $\delta V_\parallel'$, i.e., $\delta\omega \equiv |\delta\omega|\exp(i\delta\theta_k)$. Since $|\delta\omega| \sim k_\theta k_\parallel \delta V_\parallel'$, the sign of the residual stress-induced viscosity contribution is determined by

$$\chi_\phi^{Res} \sim \cos\left(\frac{\pi}{2} + \delta\theta_k - 3\theta_k\right). \tag{16}$$

ITG instability and PSFI have different mode phases, leading to different signs of χ_ϕ^{Res}. As a result, $\delta V_\parallel'$ has different effects on momentum transport in ITG and PSFI turbulence.

C. Flow profile

Although pure ITG turbulence cannot drive intrinsic flows in straight field, ∇T_{i0} affects momentum transport, and thus can regulate the flow gradient. In CSDX, the axial flow can be driven by the axial ion pressure drop. In order to uncover the ITG effect on the flow, we ignore the external sources in the following analysis. Consequently, the flow gradient within the center region of CSDX can be obtained from $\nabla\cdot\mathbf{\Pi} = 0$, where $\mathbf{\Pi}$ is the total momentum flux. Considering only the parallel Reynolds stress, the flow profile gradient can be calculated from

$$\partial_r \langle \tilde{v}_r \tilde{v}_\parallel \rangle = \partial_r(\Pi_{r\parallel}^{Res} - \chi_\phi \nabla V_\parallel) = 0. \tag{17}$$

The edge is accounted by boundary conditions for the flow. The flow profile depends heavily on the boundary condition.[9,21] The boundary layer in CSDX is controlled by coupling between ions and neutral particles. Assuming that the radial expansion of the boundary layer is negligible compared to the plasma radius, we adopt a no-slip boundary condition for $V_\parallel$. As a result, the flow profile is $V_\parallel(r) = -\int_r^a dr \nabla V_\parallel$, where a is the radius of plasma.

V. RESULTS

In this section, we present results on mode phase, $\delta V_\parallel'$ induced symmetry breaking, and flow profile, for each of the three regimes.

A. Marginal regime

When the PSF-ITG system is weakly unstable, i.e., $\Delta \gtrsim 0$, PSFI and ITG turbulence coexist. In this regime, $\nabla V_\parallel$ and ∇T_{i0} are coupled nonlinearly, and a perturbation to the mean flow profile raises the PSFI level and thus enhances the flow dissipation.

We can obtain the linear thresholds for ITG and PSFI turbulence. The PSF-ITG system can be viewed as an ITG system in the presence of $\nabla V_\parallel$. From the criterion Eq. (5), ∇T_{i0} can drive instability with a threshold depending on $\nabla V_\parallel$

$$\omega_{T,\mathrm{crit}}^2(\nabla V_\parallel) = \frac{4\tau^2 k_\parallel^2 c_s^2 (C_0 - V')^3}{27A}. \tag{18}$$

In the marginal state, i.e., $\omega_T^2 \gtrsim \omega_{T,\mathrm{crit}}^2$, the growth rate and real frequency are

$$\gamma_k \cong \frac{\sqrt{3}}{3}\frac{|k_\parallel c_s|^{2/3}}{(2A\tau)^{1/3}}\frac{\sqrt{\omega_T^2 - \omega_{T,\mathrm{crit}}^2}}{|\omega_T|^{2/3}}, \tag{19}$$

$$\omega_k \cong -\frac{|k_\parallel c_s|^{2/3}|\omega_T|^{1/3}}{(2A\tau)^{1/3}}. \tag{20}$$

Meanwhile, the PSF-ITG system can also be viewed as a PSFI system modified by ∇T_{i0}. From the criterion Eq. (5), the PSFI threshold can be obtained, and is

$$|V_\parallel'|_{\mathrm{crit}} = \frac{|k_\parallel c_s|}{k_\theta \rho_s}\left[C_0 - 3A^{1/3}\left(\frac{|\omega_T|}{2\tau|k_\parallel c_s|}\right)^{2/3}\right]. \tag{21}$$

The growth rate, $\gamma_k \sim \sqrt{|V_\parallel'| - |V_\parallel'|_{\mathrm{crit}}}$, depends *nonlinearly* on $\nabla V_\parallel$. ∇T_{i0} enhances PSFI by lowering the PSFI threshold. Therefore, in the marginal regime, PSFI and ITG instability coexist, and one can view this weakly unstable turbulence in two equivalent ways: (1) ITG turbulence modified by $\nabla V_\parallel$ and (2) PSFI turbulence modified by ∇T_{i0}.

The residual stress and turbulent viscosity are

$$\Pi_{r\parallel}^{Res} \cong -\frac{2\sqrt{3}}{3}\sum_k \frac{(2A)^{2/3}}{\tau^{1/3}|k_\parallel c_s|^{4/3}}\frac{\sqrt{\omega_T^2 - \omega_{T,\mathrm{crit}}^2}}{|\omega_T|^{2/3}} k_\theta k_\parallel \rho_s c_s |\phi_k|^2, \tag{22}$$

$$\chi_\phi \cong \frac{\sqrt{3}}{3}\sum_k \frac{(2A\tau)^{1/3}}{|k_\parallel c_s|^{2/3}}\frac{\sqrt{\omega_T^2-\omega_{T,\mathrm{crit}}^2}}{|\omega_T|^{4/3}}k_\theta^2\rho_s^2|\phi_k|^2. \quad (23)$$

$\nabla V_\parallel$ and ∇T_{i0} are coupled nonlinearly in $\Pi_{r\parallel}^{Res}$, via $\sqrt{\omega_T^2-\omega_{T,\mathrm{crit}}^2}$. Therefore, $\Pi_{r\parallel}^{Res}$ *cannot in general be decomposed into the sum of a* ∇T_{i0} *driven piece and a* $\nabla V_\parallel$ *driven piece*. Here, it is the frequency shift $\sqrt{\omega_T^2-\omega_{T,\mathrm{crit}}^2}$ which determines the instability and thus sets the residual stress and χ_ϕ.

The residual stress requires symmetry breaking. A perturbation to the mean flow gradient, $\delta V_\parallel'$, breaks the $k_\parallel \to -k_\parallel$ symmetry. As shown by Eq. (18), modes with $k_\theta k_\parallel \delta V_\parallel' > 0$ have lower $\omega_{T,\mathrm{crit}}^2$ than others. Therefore, these modes grow faster because $\gamma_k \sim \sqrt{\omega_T^2-\omega_{T,\mathrm{crit}}^2}$. As a result, a spectral imbalance in $k_\theta k_\parallel$ space is induced. For example, for $V_\parallel' < 0$, modes in the $k_\theta k_\parallel < 0$ domain have higher intensities. Therefore, the correlator is set to be $\langle k_\theta k_\parallel\rangle < 0$. Further, the residual stress is set by the spectral imbalance as

$$\Pi_{r\parallel}^{Res} \cong \frac{2\sqrt{3}}{3}\sum_{\{k|k_\theta k_\parallel<0\}}\frac{(2A)^{2/3}}{\tau^{1/3}|k_\parallel c_s|^{4/3}}\frac{\sqrt{\omega_T^2-\omega_{T,\mathrm{crit}}^2}}{|\omega_T|^{2/3}} \times |k_\theta k_\parallel|\rho_s c_s I_k\left(\delta V_\parallel'\right), \quad (24)$$

where $I_k(\delta V_\parallel') \equiv |\phi_k|^2 - |\phi_{-k}|^2$ accounts for the turbulence intensity difference and so the summation is only over the domain where $k_\theta k_\parallel < 0$.

This symmetry breaking mechanism induces a positive increment to the turbulent viscosity. $\delta V_\parallel'$ raises the PSFI level, and so enhances the turbulent viscosity. We consider the response of $\Pi_{r\parallel}^{Res}$ in the presence of a test flow shear $\delta V_\parallel'$. The perturbed complex mode frequency due to $\delta V_\parallel'$ is

$$\delta\omega \cong e^{i\delta\theta_k}\frac{\sqrt{3}}{2C_0}\frac{|k_\parallel c_s|^{2/3}}{(2A\tau)^{1/3}}\frac{\omega_{T,\mathrm{crit}}^2}{|\omega_T|^{2/3}\sqrt{\omega_T^2-\omega_{T,\mathrm{crit}}^2}}\frac{k_\theta k_\parallel \rho_s c_s \delta V_\parallel'}{k_\parallel^2 c_s^2}, \quad (25)$$

with perturbed mode phase $\delta\theta_k = \pi/2$. $\delta\theta_k$ is the same as the PSFI mode phase, indicating that $\delta V_\parallel'$ enhances PSFI turbulence. The mode phase in this regime can be obtained from the complex frequency, which is

$$\omega \cong e^{i\theta_k}\frac{|k_\parallel c_s|^{2/3}}{(2A\tau)^{1/3}}\frac{\sqrt{4\omega_T^2-\omega_{T,\mathrm{crit}}^2}}{\sqrt{3}|\omega_T|^{2/3}}, \quad (26)$$

with mode phase $\theta_k = \pi - \epsilon$ where $\epsilon \equiv \arctan\sqrt{(\omega_T^2-\omega_{T,\mathrm{crit}}^2)/3\omega_T^2} \gtrsim 0$. As a result, the residual stress in response to $\delta V_\parallel'$ can be written as a diffusive momentum flux $\delta\Pi_{r\parallel}^{Res} = -\chi_\phi^{Res}\delta V_\parallel'$ with viscosity $\chi_\phi^{Res} \sim \cos(\pi/2+\delta\theta_k-3\theta_k) = \cos(3\epsilon) > 0$. This means *the residual stress induces a positive increment to the turbulent viscosity*. Following the same calculation procedure as in Ref. 9, we can obtain the residual stress in terms of $\nabla V_\parallel$ and $\delta V_\parallel'$, which is $\Pi_{r\parallel}^{Res}(\nabla V_\parallel + \delta V_\parallel') = \Pi_{r\parallel}^{Res}(\nabla V_\parallel) - \chi_\phi^{Res}\delta V_\parallel'$, with

$$\chi_\phi^{Res} \cong \frac{4^{4/3}}{3^{5/2}}\sum_k \frac{C_0^2}{A^{1/3}}\frac{\tau^{5/3}}{|\omega_T|^{2/3}}\frac{k_\theta^2\rho_s^2|k_\parallel c_s|^{2/3}}{\sqrt{\omega_T^2-\omega_{T,\mathrm{crit}}^2}}|\phi_k|^2. \quad (27)$$

Therefore, $\delta V_\parallel'$ *enhances flow dissipation*.

One can also consider the rise in flow dissipation in terms of parallel Reynolds power density. The parallel Reynolds power density is defined as $P_\parallel^R \equiv \langle \tilde{v}_r\tilde{v}_\parallel\rangle V_\parallel'$. It accounts for the rate of energy coupled from fluctuations to mean parallel flow. When $P_\parallel^R > 0$, mean flow gains energy from fluctuations, and vice versa. The perturbed Reynolds power due to $\delta V_\parallel'$ is then $\delta P_\parallel^R = (-\chi_\phi\delta V_\parallel' + \delta\Pi_{r\parallel}^{Res})V_\parallel' = -(\chi_\phi + \chi_\phi^{Res})V_\parallel'\delta V_\parallel'$. Assuming that $\delta V_\parallel'$ has the same sign as $V_\parallel'$, $\chi_\phi^{Res} > 0$ increases the rate at which energy is coupled from mean flow to fluctuations. Thus, flow dissipation is enhanced.

Although the marginal pure ITG turbulence cannot drive intrinsic flows in a straight field, it can influence the flow profile driven by external sources. The final flow profile set by ITG turbulence can be obtained from Eq. (17), which is $\nabla V_\parallel = \Pi_{r\parallel}^{Res}/\chi_\phi$. Because $\nabla V_\parallel$ and ∇T_{i0} are nonlinearly coupled via the frequency shift $\sqrt{\omega_T^2-\omega_{T,\mathrm{crit}}^2}$, their effects on the residual stress cannot be separated. *However, the nonlinear dependence on* $\nabla V_\parallel$ *cancels, via the ratio between* $\Pi_{r\parallel}^{Res}$ *and* χ_ϕ. In order to see the flow profile's scaling with ∇T_{i0}, the factors induced by symmetry breaking effects are ignored. As a result, the estimated residual stress is

$$|\Pi_{r\parallel}^{Res}| \approx \frac{2\sqrt{3}}{3}\sum_k \frac{(2A)^{2/3}}{\tau^{1/3}|k_\parallel c_s|^{4/3}}\frac{\sqrt{\omega_T^2-\omega_{T,\mathrm{crit}}^2}}{|\omega_T|^{2/3}}|k_\theta k_\parallel|\rho_s c_s|\phi_k|^2, \quad (28)$$

which is an upper limit for $\Pi_{r\parallel}^{Res}$ since $|\sum_k k_\theta k_\parallel|\phi_k|^2| \le \sum_k |k_\theta k_\parallel||\phi_k|^2$. The fluctuation intensity, $|\phi_k|^2$, enters both $\Pi_{r\parallel}^{Res}$ and χ_ϕ, and so drops out of their ratio. Therefore, the parallel flow gradient emerges as

$$|V_\parallel'| = \frac{|\Pi_{r\parallel}^{Res}(\nabla V_\parallel, \nabla T_{i0})|}{\chi_\phi(\nabla V_\parallel, \nabla T_{i0})} \sim 2^{4/3}A^{1/3}\left(\frac{|\omega_T|}{\tau|k_\parallel c_s|}\right)^{2/3}\frac{|k_\parallel|c_s}{k_\theta\rho_s}. \quad (29)$$

The above scaling of $\nabla V_\parallel$ can be illustrated on a back-of-envelope level. Given by Eqs. (13) and (14), the ITG residual stress and turbulent viscosity scale as $\Pi_{r\parallel}^{Res} \sim \Re(i\omega_T/\tau\omega^2)$ and $\chi_\phi \sim \Re(i/\tau\omega)$, where $\omega \equiv \omega_k + i\gamma_k$ is the complex mode frequency, and $\omega_T \equiv k_\theta\rho_s c_s/L_T$ is the ion drift frequency. For ITG turbulence, $\gamma_k \sim |\omega_k| \sim (|\omega_T|/\tau)^{2/3}$. Therefore, the flow gradient scales as $\nabla V_\parallel \sim \Pi_{r\parallel}^{Res}/\chi_\phi \sim (|\omega_T|/\tau)^{2/3}|k_\parallel c_s|^{1/3}$.

B. ITG regime

Now we consider ITG turbulence well above threshold ($\omega_T^2 \gg \omega_{T,\mathrm{crit}}^2$) with the $\nabla V_\parallel$ effect as a first order correction. In this regime, a test flow shear $\delta V_\parallel'$ induces a negative correction to the viscosity. However, unlike the case of electron drift wave (EDW) turbulence, the total viscosity in ITG turbulence is positive definite. Therefore, *no intrinsic flow can be driven by ITG turbulence without symmetry breaking due to the magnetic configuration*. The difference in flow dissipations between EDW and ITG turbulence raises the question: is flow reversal possible in CSDX? Even though the answer seems to be negative, it suggests that speculations about flow reversal can be tested in fundamental plasma experiments.

The residual stress can be obtained using the growth rate and frequency, which are

$$\gamma_k \cong \frac{\sqrt{3}}{2}\frac{|\omega_T|^{1/3}|k_\parallel c_s|^{2/3}}{(\tau A)^{1/3}}\left[1-\left(\frac{\omega_{T,\mathrm{crit}}}{2|\omega_T|}\right)^{2/3}\right], \tag{30}$$

$$\omega_k \cong -\frac{1}{2}\frac{|\omega_T|^{1/3}|k_\parallel c_s|^{2/3}}{(\tau A)^{1/3}}\left[1+\left(\frac{\omega_{T,\mathrm{crit}}}{2|\omega_T|}\right)^{2/3}\right]. \tag{31}$$

The leading order complex mode frequency is

$$\omega \cong e^{i2\pi/3}\frac{|\omega_T|^{1/3}|k_\parallel c_s|^{2/3}}{(\tau A)^{1/3}}, \tag{32}$$

with mode phase $\theta_k = 2\pi/3$. Therefore, the residual stress and turbulent viscosity in this regime are

$$\Pi_{r\parallel}^{Res} \cong -\frac{\sqrt{3}}{2}\sum_k \frac{|\omega_T|^{1/3}A^{2/3}}{\tau^{1/3}|k_\parallel c_s|^{4/3}}k_\theta k_\parallel \rho_s c_s|\phi_k|^2, \tag{33}$$

$$\chi_\phi \cong \frac{\sqrt{3}}{2}\sum_k \frac{(\tau A)^{1/3}}{|\omega_T|^{1/3}|k_\parallel c_s|^{2/3}}k_\theta^2\rho_s^2|\phi_k|^2. \tag{34}$$

$\delta V_\parallel'$ induces a negative viscosity increment. Similar to the case of marginal regime, the residual stress is set by the spectral imbalance, which, given a flow shear $\delta V_\parallel' < 0$, is

$$\Pi_{r\parallel}^{Res} \cong \frac{\sqrt{3}}{2}\sum_{\{k|k_\theta k_\parallel<0\}} \frac{|\omega_T|^{1/3}A^{2/3}}{\tau^{1/3}|k_\parallel c_s|^{4/3}}|k_\theta k_\parallel|\rho_s c_s I_k\left(\delta V_\parallel'\right). \tag{35}$$

The perturbed complex mode frequency due to a test flow shear $\delta V_\parallel'$ is

$$\delta\omega = e^{i\pi/3}\left(\frac{\tau}{|\omega_T|}\right)^{1/3}\frac{k_\theta k_\parallel \rho_s c_s \delta V_\parallel'}{3A^{2/3}|k_\parallel c_s|^{2/3}}, \tag{36}$$

with the perturbed mode phase $\delta\theta_k = \pi/3$. Since ITG instability is well established (i.e., $\omega_T^2 \gg \omega_{T,\mathrm{crit}}^2$), the test flow shear not only perturbs the growth rate, but also affects the real frequency. Therefore, the perturbed mode phase carries features of both PSFI and ITG mode phases. Since $\chi_\phi^{Res} \sim \cos(3\theta_k - \delta\theta_k - \pi/2) = \cos(5\pi/6) < 0$, the residual stress induces a negative viscosity increment, which is

$$\chi_\phi^{Res} = -\frac{\sqrt{3}}{6}\sum_k \frac{(\tau A)^{1/3}}{|\omega_T|^{1/3}|k_\parallel c_s|^{2/3}}k_\theta^2\rho_s^2|\phi_k|^2. \tag{37}$$

This negative viscosity increment reduces the rate of energy coupling from the mean flow profile to fluctuations, since the Reynolds power density due to $\delta V_\parallel'$ in this case is $\delta P_\parallel^{Res} = -(\chi_\phi - |\chi_\phi^{Res}|)V_\parallel'\delta V_\parallel'$. Therefore, $\delta V_\parallel'$ *reduces* flow dissipation, and so can *enhance* the flow gradient, since $\nabla V_\parallel \sim \Pi_{r\parallel}^{Res}/\chi_\phi$.

However, $\delta V_\parallel'$ *cannot self-amplify, although it induces a negative viscosity increment*. The dynamics of $\delta V_\parallel$ is determined by $\partial_t \delta V_\parallel' = \chi_\phi^{Tot}\partial_r^2 \delta V_\parallel'$, with growth rate $\gamma_q = -q_r^2\chi_\phi^{Tot}$. Here, the *total* viscosity, $\chi_\phi^{Tot} = \chi_\phi - |\chi_\phi^{Res}|$, is *positive definite*, because $|\chi_\phi^{Res}| = \frac{1}{3}\chi_\phi$, which can be obtained by comparing Eqs. (34) and (37). *Since* $\chi_\phi^{Tot} > 0$, *the growth rate* γ_q *is negative, so the flow shear modulation is damped*. This is also shown by the Reynolds power density. Since $\chi_\phi^{Tot} > 0$, the Reynolds power density is negative, and thus *energy is coupled from a mean flow profile to fluctuations*, although at a reduced rate due to $\chi_\phi^{Res} < 0$. Table I summarizes the comparison between $\delta V_\parallel'$ induced symmetry breaking in ITG turbulence and electron drift wave turbulence.

In order to calculate the flow profile, we need to eliminate the residual stress' nonlinearity in $\nabla V_\parallel$. In the ITG regime, $\nabla V_\parallel$ effects can decouple from ∇T_{i0}. This is because ∇T_{i0} is well above the stability boundary, and dominates over $\nabla V_\parallel$ in magnitude. Moreover, the residual stress induces an negative viscosity increment χ_ϕ^{Res}. Therefore, the residual stress can be linearized as

$$\Pi_{r\parallel}^{Res}(\nabla T_{i0}, \delta V_\parallel') \approx \Pi_{r\parallel}^{Res}(\nabla T_{i0}) + |\chi_\phi^{Res}(\nabla T_{i0})|\delta V_\parallel'. \tag{38}$$

The up-gradient component results from the symmetry breaking by $\delta V_\parallel'$.

The negative incremental viscosity χ_ϕ^{Res} induced by the residual stress regulates the transport of mean flow. Therefore, in response to a mean flow gradient, the residual stress can induce an up-gradient momentum flux, i.e., $\Pi_{r\parallel}^{Res}(\nabla T_{i0}, V_\parallel') \approx \Pi_{r\parallel}^{Res}(\nabla T_{i0}) + |\chi_\phi^{Res}|V_\parallel'$. This leads to Eq. (39), which calculates the mean flow gradient. Such "negative viscosity" phenomena are well known in geophysical fluid dynamics and magnetized plasmas.

With $\Pi_{r\parallel}^{Res}(\nabla T_{i0})$, $\chi_\phi(\nabla T_{i0})$ and $\chi_\phi^{Res}(\nabla T_{i0})$ given by Eqs. (33), (34), and (37), the flow gradient is

$$|V_\parallel'| = \frac{|\Pi_{r\parallel}^{Res}(\nabla T_{i0})|}{\chi_\phi(\nabla T_{i0}) - |\chi_\phi^{Res}(\nabla T_{i0})|} \sim \frac{3}{2}A^{1/3}\left(\frac{|\omega_T|}{\tau|k_\parallel c_s|}\right)^{2/3}\frac{|k_\parallel|c_s}{k_\theta\rho_s}. \tag{39}$$

Eq. (39) is an upper bound for the intrinsic $V_\parallel'$ driven by ITG turbulence. Again, $\nabla V_\parallel$ follows the general trend revealed by scalings of Eqs. (13) and (14), i.e., $\nabla V_\parallel \sim (|\omega_T|/\tau)^{2/3}|k_\parallel c_s|^{1/3}$.

Can there be flow reversal in CSDX, given the different effects of ITG and EDW turbulence on momentum transport? In tokamaks, reversal refers to the phenomenon, where the global toroidal rotation profile spontaneously changes direction. The rotation direction flips when density increases and exceeds n_{sat}, the critical density that triggers the transition from the linear ohmic confinement (LOC) to saturated ohmic confinement (SOC) regime. Also, hysteresis is observed as density is ramped down and the rotation direction flips back. The LOC to SOC transition is thought to be triggered by a change in turbulence population from trapped electron mode (TEM) to ITG. Thus, it is speculated that the Ohmic reversal is due to a change in the sign of $\Pi_{r\|}^{Res}$ triggered when the collisionality $\nu^* > \nu^*_{crit}$, which corresponds to $n > n_{sat}$, tending to drive the turbulence to ITG. Recent simulations show that a flip in the sign of $\Pi_{r\|}^{Res}$ can occur in the weak shear regime.[22]

One wonders if these speculations about flow reversal can be tested in basic plasma experiments. The positive definite χ_ϕ^{Tot} in ITG turbulence, in both weakly and strongly unstable regimes, suggests that flow reversal-by a change in the mode type from electron drift wave (EDW) to ITG-seems unlikely in CSDX. With no-slip boundary condition, the flow profile in CSDX is calculated in Ref. 9, which is

$$V_\| = \int_r^a dr \frac{a\Delta P_i}{2\rho_0 L \chi_\phi^{\mathrm{Tot}}}. \tag{40}$$

Here, ΔP_i is the ion pressure drop in the axial direction induced by the plasma heating on one end of the cylindrical tube. ρ_0 is plasma density and L is the axial length of the tube. When the major mode type flips between EDW and ITG, the direction of pressure drop doesn't change, so the direction of flow depends on the sign of total viscosity, i.e., $V_\| \sim 1/\chi_\phi^{Tot}$. It should be noted that in the realistic ITG regime of CSDX, the ITG residual stress may be weak, compared to external flow drives. Thus, we view the axial ΔP_i as the main flow drive in the ITG regime here. In EDW, χ_ϕ^{Tot} is kept positive by the PSFI contribution, i.e., $\chi_\phi^{Tot} = \chi_\phi^{EDW} + \chi_\phi^{PSFI} - |\chi_\phi^{Res}| > 0$. Note that the nonlinear dependence of χ_ϕ^{Tot} on $\nabla V_\|$ determines the magnitude of a saturated flow gradient. In marginal ITG turbulence, $\chi_\phi^{Res} > 0$ so χ_ϕ^{Tot} is positive. Also, when ITG turbulence is well above the linear threshold, even though $\delta V_\|'$ drives $\chi_\phi^{Res} < 0$, the *total* viscosity, $\chi_\phi^{Tot} = \chi_\phi - |\chi_\phi^{Res}|$, remains positive since $|\chi_\phi^{Res}|/\chi_\phi = 1/3$. Therefore, in ITG turbulence, χ_ϕ^{Tot} is positive definite. As a result, when the mode type flips from EDW to ITG, the sign of χ_ϕ^{Tot} does not change, and so the flow does not reverse.

C. PSFI regime

In CSDX, $\nabla V_\|$ can be driven and enhanced by various external sources. When the flow gradient is above the PSFI regime boundary, PSFI controls the turbulence. Note that the PSFI regime boundary ($|V_\|'|_{\mathrm{reg}}$) is above the linear PSFI threshold ($|V_\|'|_{\mathrm{crit}}$). In the PSFI regime, both PSFI and ITG instability are above their linear instability thresholds. Due to the PSFI relaxation, the flow profile gradient saturates at $|V_\|'|_{\mathrm{reg}}$, i.e., $|V_\|'|_{\mathrm{crit}} \ll |V_\|'| \sim |V_\|'|_{\mathrm{reg}} \sim (\nabla T_{i0})^{2/3}$.

The turbulent viscosity by PSFI turbulence is nonlinear in $\nabla V_\|$, which leads to the saturation of flow gradient. The growth rate and real frequency in the PSFI regime are

$$\gamma_k \cong \frac{|k_\| c_s|}{\sqrt{A}} \sqrt{V' - C_0}, \tag{41}$$

$$\omega_k \cong -\frac{|\omega_T|}{2\tau(V' - C_0)}. \tag{42}$$

The growth rate is nonlinear in $\nabla V_\|$, while the real frequency is negative as a result of ∇T_{i0} effects. Hence, the turbulent viscosity is

$$\chi_\phi = \sum_k \frac{\sqrt{A}}{|k_\| c_s| \sqrt{V' - C_0}} k_\theta^2 \rho_s^2 |\phi_k|^2. \tag{43}$$

The nonlinear dependence of χ_ϕ on $\nabla V_\|$ indicates that the flow gradient can saturate. As a result, $|V_\|'|$ *saturates at the PSFI regime boundary which is above the linear PSFI threshold* (Fig. 3), i.e.

$$|V_\|'| \approx |V_\|'|_{\mathrm{reg}} = \frac{3}{2^{2/3}} A^{1/3} \left(\frac{|\omega_T|}{\tau |k_\| c_s|} \right)^{2/3} \frac{|k_\| c_s|}{k_\theta \rho_s}. \tag{44}$$

Therefore, the saturated flow gradient is *above* the linear PSFI threshold, and grows with ∇T_{i0} as shown by Eq. (44), i.e., $|V_\|'|_{\mathrm{crit}}/|k_\| c_s| \ll |V_\|'|/|k_\| c_s| \sim |\nabla T_{i0}|^{2/3}/(k_\| T_{i0})^{2/3}$.

VI. DISCUSSION

In this paper, we have explored the physics of axial flow generation in ITG turbulence, and of axial flow stiffness. The main results in this paper are as follows:

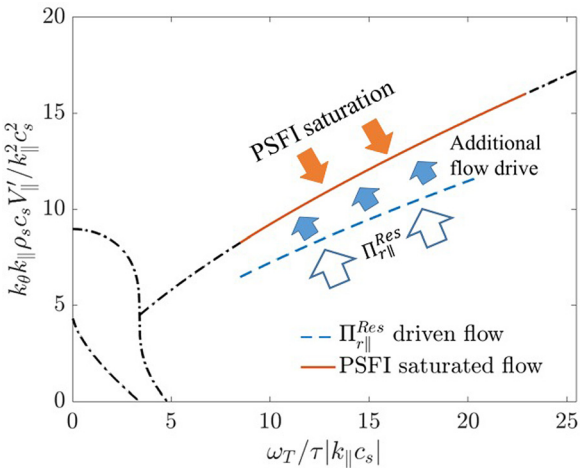

FIG. 3. The additional flow drive can push the flow across the PSFI threshold, triggering nonlinear PSFI relaxation. The flow gradient is then kept near the PSFI regime boundary as a result of balancing between PSFI saturation and total flow drive.

- We have shown that pure ITG turbulence cannot drive intrinsic flows in a straight magnetic field, but can induce a negative viscosity *increment*, which reduces the turbulent flow dissipation.
- PSFI saturates the flow gradient, when $\nabla V_\parallel$ is driven above the PSFI regime boundary.
- The flow gradient saturates at the PSFI regime boundary, which is above the PSFI linear threshold and tracks the ITG drive, i.e., $\nabla V_\parallel/|k_\parallel c_s| \sim (\nabla T_{i0})^{2/3}/(k_\parallel T_{i0})^{2/3}$.

Below we discuss these results.

Negative compressibility leads to a negative viscosity increment in a straight magnetic field. When the ITG turbulence is well above its stability boundary, a perturbation to the flow gradient $\delta V_\parallel'$ results in a negative viscosity increment, $\chi_\phi^{Res} < 0$. The total viscosity is then reduced, i.e., $\chi_\phi^{Tot} = \chi_\phi - |\chi_\phi^{Res}|$. However, $\delta V_\parallel'$ cannot reinforce itself because χ_ϕ^{Tot} is always positive (since $|\chi_\phi^{Res}| = \frac{1}{3}\chi_\phi$). This means that in order to drive an intrinsic flow, $\Pi_{r\parallel}^{Res}$ requires other symmetry breaking mechanisms that likely involve magnetic shear. Therefore, there is no intrinsic flow driven by pure ITG turbulence in straight fields. In CSDX, axial flows can be driven by various external drives, e.g., end plate biasing and axial ion pressure drop.

In straight magnetic fields, the flow gradient can saturate due to PSFI relaxation. The flow gradient in CSDX can be enhanced by various external sources. When $\nabla V_\parallel$ steepens enough, so that PSFI drive dominates over ITG drive, flow gradient saturates by PSFI relaxation. PSFI is nonlinear in $\nabla V_\parallel$, and so is the viscosity driven by PSFI turbulence. Consequently, $\nabla V_\parallel$ saturates at the PSFI regime boundary (which is above the linear PSFI threshold) and grows as $\nabla V_\parallel \sim (\nabla T_{i0})^{2/3}$. This scaling of flow gradient implies a generalized Rice-type scaling, i.e., $\nabla V_\parallel \sim (\nabla T_{i0})^{\alpha}$, with $\alpha = 2/3$.

We can also solve for the saturated flow gradient from Eq. (40). The PSFI saturation effect can be accommodated in Eq. (40) by introducing the PSFI induced turbulent viscosity χ_ϕ^{PSFI} (given by Eq. (43)) when the flow shear is above the PSFI stability boundary. As a result, the total viscosity is

$$\chi_\phi^{Tot} = \begin{cases} \chi_\phi^{ITG} - \chi_\phi^{Res} & \text{if } |V_\parallel'| < |V_\parallel'|_{\text{crit}} \\ \chi_\phi^{ITG} + \chi_\phi^{PSFI} - \chi_\phi^{Res} & \text{if } |V_\parallel'| \geq |V_\parallel'|_{\text{crit}}. \end{cases} \quad (45)$$

Hence, Eq. (40) becomes a nonlinear equation for $\nabla V_\parallel$, due to the contribution of χ_ϕ^{PSFI}. Since χ_ϕ^{PSFI} is nonlinear in $\nabla V_\parallel$, it becomes very strong compared to $\chi_\phi^{ITG} - \chi_\phi^{Res}$ when PSFI is sufficiently excited. Therefore, the flow gradient solved from Eq. (40) saturates at the PSFI regime boundary.

This generalized scaling of $\nabla V_\parallel$ with ∇T_{i0} indicates that the interaction between the flow profile and the turbulence drive exhibits simple trends. In ITG turbulence, $\nabla V_\parallel$ and ∇T_{i0} are coupled nonlinearly. But due to the ITG residual stress and PSFI saturation, their final states are constrained by the scaling $\nabla V_\parallel \sim (\nabla T_{i0})^{2/3}$.

Even though $\delta V_\parallel'$ has different effects on electron drift wave (EDW) and ITG turbulence, flow reversal by changing the mode from EDW to ITG seems unlikely. As is known, the axial flow in CSDX is driven by ion pressure drop in the axial direction (ΔP_i), which is $V_\parallel \sim \int_r^a \Delta P_i/\chi_\phi^{Tot}$. In EDW, the negative viscosity increment induced by $\delta V_\parallel'$ can turn the total viscosity negative in some transient state, i.e., $\chi_\phi^{Tot} = \chi_\phi - |\chi_\phi^{Res}| < 0$. Nevertheless, in the final state, the self-amplification of a test flow shear is saturated by PSFI, so the total viscosity remains positive due to the PSFI contribution, i.e., $\chi_\phi^{Tot} = \chi_\phi^{EDW} + \chi_\phi^{PSFI} - |\chi_\phi^{Res}| > 0$. When ITG turbulence is excited, χ_ϕ^{Tot} driven by ITG is positive definite. Thus, for the same flow boundary condition, the sign of χ_ϕ^{Tot} does not change, despite change in mode. Therefore, flow reversal in CSDX will *not* track changes in turbulence.

The following works are proposed for the future. They address remaining issues about flow generation and saturation in CSDX. First, ion-neutral coupling mostly occurs in the boundary layer in CSDX, where plasmas are partially ionized. However, it sets the boundary condition for parallel flows, and thus affects the global flow structure. Since the flow profile is very sensitive to the boundary condition, ion-neutral coupling is of great interest. Second, coupling between perpendicular flow and parallel flow. In tokamaks, poloidal flow and toroidal flow are coupled by sheared magnetic fields. Even though CSDX has straight field lines, the parallel flow gradient ($\nabla V_\parallel$) can be coupled to the perpendicular flow gradient ($\nabla V_\perp$) via the turbulence.[23] Particularly, a sheared perpendicular flow can saturate the parallel flow gradient in CSDX. Because both $\nabla V_\perp$ and $\nabla V_\parallel$ are driven by the background turbulence, their magnitudes are limited by Reynolds power density, which measures the rate at which fluctuations transfer energy to mean flows. The coupling between perpendicular and parallel flows can also be viewed as an extended predator-prey model[24,25] in which $\nabla V_\perp$ and $\nabla V_\parallel$ are two predators (perhaps hierarchical) and the turbulence is the prey. Third, reversal dynamics remains an open question. As is known, flow reversal is unlikely in CSDX by changing the mode from electron drift wave (EDW) to ITG, because PSFI saturation of $\nabla V_\parallel$ in EDW turbulence keeps the total viscosity positive. However, $\nabla V_\perp$ saturation complicates the problem of flow reversal. The bottom line is that such predictions for flow reversal can be tested in basic plasma experiments.

ACKNOWLEDGMENTS

The authors are grateful to R. Hong, G. R. Tynan, W. X. Wang, J. E. Rice, and X. Q. Xu for useful discussions. P. H. Diamond thanks the participants in the 2013 and 2015 Festival de Théorie for many useful and interesting discussions. This work was supported by the U.S. Department of Energy, Office of Science, OFES, under Award No. DE-FG02-04ER54738, and CMTFO Award No. DE-SC0008378.

[1]H. Reimerdes, T. C. Hender, S. A. Sabbagh, J. M. Bialek, M. S. Chu, A. M. Garofalo, M. P. Gryaznevich, D. F. Howell, G. L. Jackson, R. J. La Haye *et al.*, Phys. Plasmas **13**, 056107 (2006).

[2]E. J. Synakowski, S. H. Batha, M. A. Beer, M. G. Bell, R. E. Bell, R. V. Budny, C. E. Bush, P. C. Efthimion, T. S. Hahm, G. W. Hammett *et al.*, Phys. Plasmas **4**, 1736 (1997).
[3]B. W. Rice, T. S. Taylor, K. H. Burrell, T. A. Casper, C. B. Forest, H. Ikezi, L. L. Lao, E. A. Lazarus, M. E. Mauel, B. W. Stallard *et al.*, Plasma Phys. Controlled Fusion **38**, 869 (1996).
[4]M. Yoshida, M. Honda, E. Narita, N. Hayashi, H. Urano, M. Nakata, N. Miyato, H. Takenaga, S. Ide, and Y. Kamada, Nucl. Fusion **55**, 073014 (2015).
[5]P. Mantica, C. Angioni, C. Challis, G. Colyer, L. Frassinetti, N. Hawkes, T. Johnson, M. Tsalas, P. C. deVries, J. Weiland *et al.*, Phys. Rev. Lett. **107**, 135004 (2011).
[6]J. E. Rice, J. W. Hughes, P. H. Diamond, Y. Kosuga, Y. A. Podpaly, M. L. Reinke, M. J. Greenwald, O. D. Gürcan, T. S. Hahm, A. E. Hubbard *et al.*, Phys. Rev. Lett. **106**, 215001 (2011).
[7]S. Thakur, C. Brandt, L. Cui, J. Gosselin, A. Light, and G. Tynan, Plasma Sources Sci. Technol. **23**, 044006 (2014).
[8]P. H. Diamond, Y. Kosuga, Ö. D. Gürcan, C. J. McDevitt, T. S. Hahm, N. Fedorczak, J. E. Rice, W. X. Wang, S. Ku, J. M. Kwon *et al.*, Nucl. Fusion **53**, 104019 (2013).
[9]J. C. Li, P. H. Diamond, X. Q. Xu, and G. R. Tynan, Phys. Plasmas **23**, 052311 (2016).
[10]P. H. Diamond, S. I. Itoh, K. Itoh, and T. S. Hahm, Plasma Phys. Controlled Fusion **47**, R35 (2005).
[11]Y. Kosuga, S. I. Itoh, and K. Itoh, Plasma Fusion Res. **10**, 3401024 (2015).
[12]J. E. Rice, A. Ince-Cushman, J. S. deGrassie, L. G. Eriksson, Y. Sakamoto, A. Scarabosio, A. Bortolon, K. H. Burrell, B. P. Duval, C. Fenzi-Bonizec *et al.*, Nucl. Fusion **47**, 1618 (2007).
[13]L. Cui, A. Ashourvan, S. C. Thakur, R. Hong, P. H. Diamond, and G. R. Tynan, Phys. Plasmas **23**, 055704 (2016).
[14]N. Mattor and P. H. Diamond, Phys. Fluids **31**, 1180 (1988).
[15]J. E. Rice, I. Cziegler, P. H. Diamond, B. P. Duval, Y. A. Podpaly, M. L. Reinke, P. C. Ennever, M. J. Greenwald, J. W. Hughes, Y. Ma *et al.*, Phys. Rev. Lett. **107**, 265001 (2011).
[16]T. S. Hahm, P. H. Diamond, Ö. D. Gürcan, and G. Rewoldt, Phys. Plasmas **14**, 072302 (2007).
[17]A. G. Peeters, C. Angioni, A. Bortolon, Y. Camenen, F. J. Casson, B. Duval, L. Fiederspiel, W. A. Hornsby, Y. Idomura, T. Hein *et al.*, Nucl. Fusion **51**, 094027 (2011).
[18]C. Angioni, Y. Camenen, F. J. Casson, E. Fable, R. M. McDermott, A. G. Peeters, and J. E. Rice, Nucl. Fusion **52**, 114003 (2012).
[19]Ö. D. Gürcan, P. H. Diamond, T. S. Hahm, and R. Singh, Phys. Plasmas (1994–present) **14**, 042306 (2007).
[20]Ö. D. Gürcan, P. H. Diamond, P. Hennequin, C. J. McDevitt, X. Garbet, and C. Bourdelle, Phys. Plasmas **17**, 112309 (2010).
[21]J. Abiteboul, P. Ghendrih, V. Grandgirard, T. Cartier-Michaud, G. Dif-Pradalier, X. Garbet, G. Latu, C. Passeron, Y. Sarazin, A. Strugarek *et al.*, Plasma Phys. Controlled Fusion **55**, 074001 (2013).
[22]Z. X. Lu, W. X. Wang, P. H. Diamond, G. Tynan, S. Ethier, C. Gao, and J. Rice, Phys. Plasmas **22**, 055705 (2015).
[23]L. Wang, P. H. Diamond, and T. S. Hahm, Plasma Phys. Controlled Fusion **54**, 095015 (2012).
[24]A. Ashourvan, P. H. Diamond, and Ö. Gürcan, Phys. Plasmas **23**, 022309 (2016).
[25]A. Ashourvan and P. H. Diamond, Phys. Rev. E **94**, 051202 (2016).